

Accessibility of Cell Wall Lignin in Solvent Extraction of Ultrathin Spruce Wood Sections

Mehedi Reza,[†] Leonardo G. Rojas,[‡] Eero Kontturi,^{‡,*} Tapani Vuorinen,[‡] and Janne Ruokolainen[†]

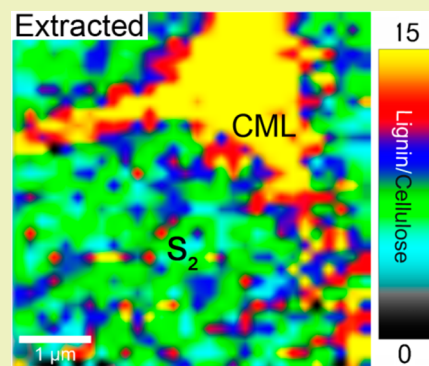
[†]Department of Applied Physics, Aalto University, P.O. Box 11100, FI-00076 Aalto, Finland

[‡]Department of Forest Products Technology, Aalto University, P.O. Box 16300, FI-00076 Aalto, Finland

S Supporting Information

ABSTRACT: Wood is a naturally occurring composite, comprising cellulose, hemicellulose, and lignin. The tightly arranged cell wall components make the fibers resistant against chemical and microbial degradation. This natural resisting power of fibers is a technical obstacle during the degradation of cellulose into sugars. Therefore, removal of cell wall lignin is necessary in order to make the cellulose accessible. In this study, ultrathin sections of Norway spruce (*Picea abies*) branch wood were examined using Raman and transmission electron microscopy (TEM) before and after extracting the sections with 1,4-dioxane without resin embedding in order to study the accessibility of native lignin. The progress of extraction of lignin was followed by measuring its Raman scattering intensity at the $\sim 1600\text{ cm}^{-1}$ band. It was found that lignin was extracted not only from the compound middle lamellae but also from other layers of the cell wall. Changes in the contrast of TEM images confirmed a decrease in lignin concentration after solvent extraction. Observed ruptures in the S_1 layer indicated that extraction weakened this layer in particular.

KEYWORDS: Lignin accessibility, Lignin distribution, Lignin extraction, Raman microscopy, TEM, Spruce wood



INTRODUCTION

Wood is a composite material with high mechanical strength. While cellulose forms the semicrystalline skeletal structure of wood fibers, it is surrounded by an amorphous matrix of hemicelluloses and lignin.¹ In addition to the supramolecular arrangement, lignin is covalently linked to many of the cell wall polysaccharides,² thus strengthening the fiber structure. Among their other functions, fibers are able to bear strong mechanical stress while resisting chemical and microbial degradation by the environment. However, this natural resistance and inertness poses a serious technical challenge to the attempts to degrade cellulose into glucose for the subsequent fermentation to ethanol, which is hoped to replace oil-based substances as transportation fuels in the future. In other words, the tight arrangement of the components in the cell wall hinders extraction of sugars and other useful compounds in the so-called biorefinery scenario.³ The presence of lignin, for example, restricts the accessibility of cellulose during various degradation efforts. Explicitly, many studies have shown a correlation between delignification and sugar release during hydrolytic lignocellulose fractionation process.^{4–6}

In most schemes for biorefinery systems, the delignification of the wood cell wall is performed by a means of severe chemical treatments, such as kraft pulping under strong alkaline conditions and high temperature.⁷ By contrast to this harsh chemical approach, it is possible to actually dissolve lignin with some specific solvents, and we feel that this approach has remained underutilized by the biorefinery community. As a first step, we have undertaken the present study where the

accessibility of lignin upon extraction by 1,4-dioxane has been investigated. In this fundamental effort, we utilized ultrathin cross sections from branches of Norway spruce. Raman microspectroscopy (RM) and transmission electron microscopy (TEM) were the chosen methods to unravel the cell wall behavior during extraction and the topochemistry of lignin after extraction. RM in particular is a valuable asset because of its ability to yield simultaneous chemical and morphological information. Moreover, in addition to the area scan, RM allows depth scans by using the motorized scan stage, although the resolution is determined by the laser wavelength, numerical aperture of the microscope objective, and refractive index of the medium. Depth profiling was not attempted in this work, and because RM has exhibited depth of detection between 8 and 20 μm ,⁸ we assumed that information over the whole thickness of our ultrathin (200 nm) wood sections would be retrieved. Furthermore, the contrast between different cell wall layers has been improved by KMnO_4 staining for TEM. Although solvent extracted lignin has been isolated and characterized,^{9–11} very few studies exist on the morphological location of the residual lignin in the cell wall after extraction.¹²

MATERIALS AND METHODS

Sample Preparation. Cubes of normal air-dried Norway spruce (*Picea abies*) branch wood were prepared without embedding and

Received: November 12, 2013

Revised: December 10, 2013

Published: December 12, 2013

without any pretreatment that could influence the extraction process. Ultrathin sections (~200 nm) were cut at cryogenic temperature (-40 °C) using an ultramicrotome (Leica EM FC7) equipped with a diamond knife. The sections were collected on copper grids.

Lignin Extraction. For extraction, grids with wood sections were placed in Petri dishes filled with 1,4-dioxane (Sigma-Aldrich). After 1 h, the grids with the sections were removed and gently washed with pure 1,4-dioxane. The short extraction time was considered to be sufficient because the sections were only ~200 nm thick.

Raman Microspectroscopy. The samples were examined with an alpha300 R confocal Raman microscope (Witec GmbH, Germany) equipped with a piezoelectric scanner at ambient conditions. A frequency doubled Nd:YAG laser (532 nm, 10 mW) was focused onto the sample using a 100× (Nikon, NA = 0.95) air objective. The excitation laser was polarized horizontally. The spectra were acquired using a CCD (DU970N-BV) behind a grating (600 grooves/mm) spectrograph (Acton, Princeton Instruments, Inc., Trenton, NJ). An integration time of 0.3 s was used for collecting each spectrum. The baseline correction was performed with WiTec project 2.10 (Witec GmbH, Germany) using a fifth order polynomial. Further smoothing to the spectra was performed using OriginPro 9.0.0 (OriginLab Corporation, Northampton, MA). Raman images were constructed by integrating characteristic bands (Table 1).

Table 1. Raman Bands of Cell Wall Polymers Used for Constructing Images¹³

polymer	Raman band (cm ⁻¹)	Raman mode
lignin	1583–1620	aromatic ring
cellulose	1120–1130	C–O stretch

In this investigation, 14 ROIs (7 unextracted + 7 extracted) randomly selected from several sections were scanned. Images of the intensity ratio between lignin and cellulose bands in the ROI were produced. The ratio images provide reliable chemical information because the artifacts caused by the surface unevenness and changes in the laser intensity are greatly reduced.¹⁴ To follow lignin extraction, average Raman spectra were produced by drawing ROIs in the S₂ layer and compound middle lamella (CML) (including cell corner middle lamellae) of the cell wall using WiTec project 2.10. Because we experienced severe section removal during the extraction process, we could not perform mapping in the same ROI before and after extraction. Original ROIs of Raman images presented in this article are available in Figure S1 of the Supporting Information.

Transmission Electron Microscopy (TEM). Wood sections were stained with 1% KMnO₄ for 30 min in citric acid buffer. The wood sections (both unextracted and extracted) for TEM were prepared under similar conditions. Therefore, it was assumed that the effect of staining with KMnO₄ will be similar on both the unextracted and the extracted sections. This staining method is specific for lignin and improves contrast between regions of variable lignin content within wood cell wall.¹⁵ The ultrathin sections were studied in a TEM (FEI Tecnai 12) at an accelerating voltage of 80 kV.

RESULTS AND DISCUSSION

Raman Microspectroscopy. RM is a vibrational spectroscopic technique that provides information about chemical composition of materials based on the analysis of the inelastic scattering of the light interacting with chemical bonds. The frequency shift observed between the incident and scattered light is assigned to a particular vibration mode of a chemical bond. Moreover, RM allows high resolution mapping (0.6–1 μm) in a nondestructive manner. RM analysis has allowed the evaluation of polymers' distribution^{14,16–18} and orientation^{19–21} in the plant cell wall. Raman spectra of model compounds have been measured to detect their applicability in studying lignocellulosic materials.^{13,22–25}

Average Raman spectra from the S₂ layer of the secondary wall and CML from unextracted and extracted sections are shown in Figure 1; lignin and cellulose have the most prominent bands and can be easily detected. Spectral features of extracted lignin from the CML and S₂ layer were also obtained by subtracting extracted spectra from unextracted one (Figure 1c,d). For the S₂ layer, subtraction was performed after normalizing unextracted and extracted spectra at the 1122 cm⁻¹ cellulose band,²¹ assuming that no cellulose was removed during extraction. In this way, we estimated that ~39% of the lignin in the S₂ layer was removed by extraction. Because no carbohydrate peaks were detected in the CML spectra, similar normalization could not be applied to them. Instead, we determined the intensity ratio of the aromatic lignin band in the CML and S₂ layer ($I_{\text{CML}}:I_{\text{S}_2}$) before and after extraction. Because the conditions during imaging of each sample were unchanged and we knew that $I_{\text{S}_2, \text{extracted}} = 0.61I_{\text{S}_2, \text{unextracted}}$, we estimated that ~46% of the lignin in the CML was extracted. These results indicate that the extent of extraction was roughly similar for both the CML and S₂ layers. Because the relative amount of condensed lignin structures is higher in the CML, it would intuitively make sense that the relative amount of extracted lignin would be lower from the CML. The condensed C–C structures, such as 5–5 and β–5 are more difficult to degrade, for example, during pulping, than the noncondensed C–O structure like β–O–4.^{27,28} There are, however, many factors that govern the extent of extraction with 1,4-dioxane, such as the amount of possible lignin–hemicellulose bonds. In this study, we concentrated mainly on the accessibility of lignin by 1,4-dioxane in ultrathin sections, and thus, the consequences could be different in case of thicker samples.

Figure 2a shows the intensity ratio I_{1600}/I_{1122} (lignin:cellulose ratio in secondary wall) of the unextracted section (Figure S2, Supporting Information); a higher intensity ratio was observed in the CML, indicating a highly lignified region previously described in the literature.^{18,29,30} This is also visible in Raman spectra presented in Figure 1a. An almost homogeneous lignin:cellulose ratio can be seen within the secondary wall, which is in agreement with the results of Hänninen et al.¹⁴ for Norway spruce wood cell wall.

A Raman image constructed according to the intensity ratio I_{1600}/I_{1122} after 1 h of extraction is depicted in Figure 2b (Figure S3, Supporting Information); significant changes in the chemical composition of the CML and secondary wall can be observed in association with a reduction in Raman scattering intensity in the lignin derived band at 1600 cm⁻¹ (Figure 1). These changes have occurred both in the secondary wall and CML. Also, Raman images showed high lignin content only in the cell corners after extraction. The changes in the Raman intensity in the spectra and color scale in the Raman images could be affected by the presence of lignans (an aromatic extractive); however, in Norway spruce, lignans are mainly present in knots (i.e., inside the stem) and decrease to a level below 1% 10–20 cm outward in the branch.^{31,32} Samples investigated in this study were collected from the straight part of branch away from the knots and contain normal sapwood.

From this study, it is apparent that lignin is extracted from all the cell wall layers but in an incomplete fashion. As the secondary wall of softwood tracheids contains most of the total cell wall lignin,³³ we assume that the extracts obtained after the treatment contain mostly secondary wall lignin. After 1 h of lignin extraction, there is a clear sign of reduction in the I_{1600}/I_{1122} intensity ratio in the CML (Figure 2). The extraction time

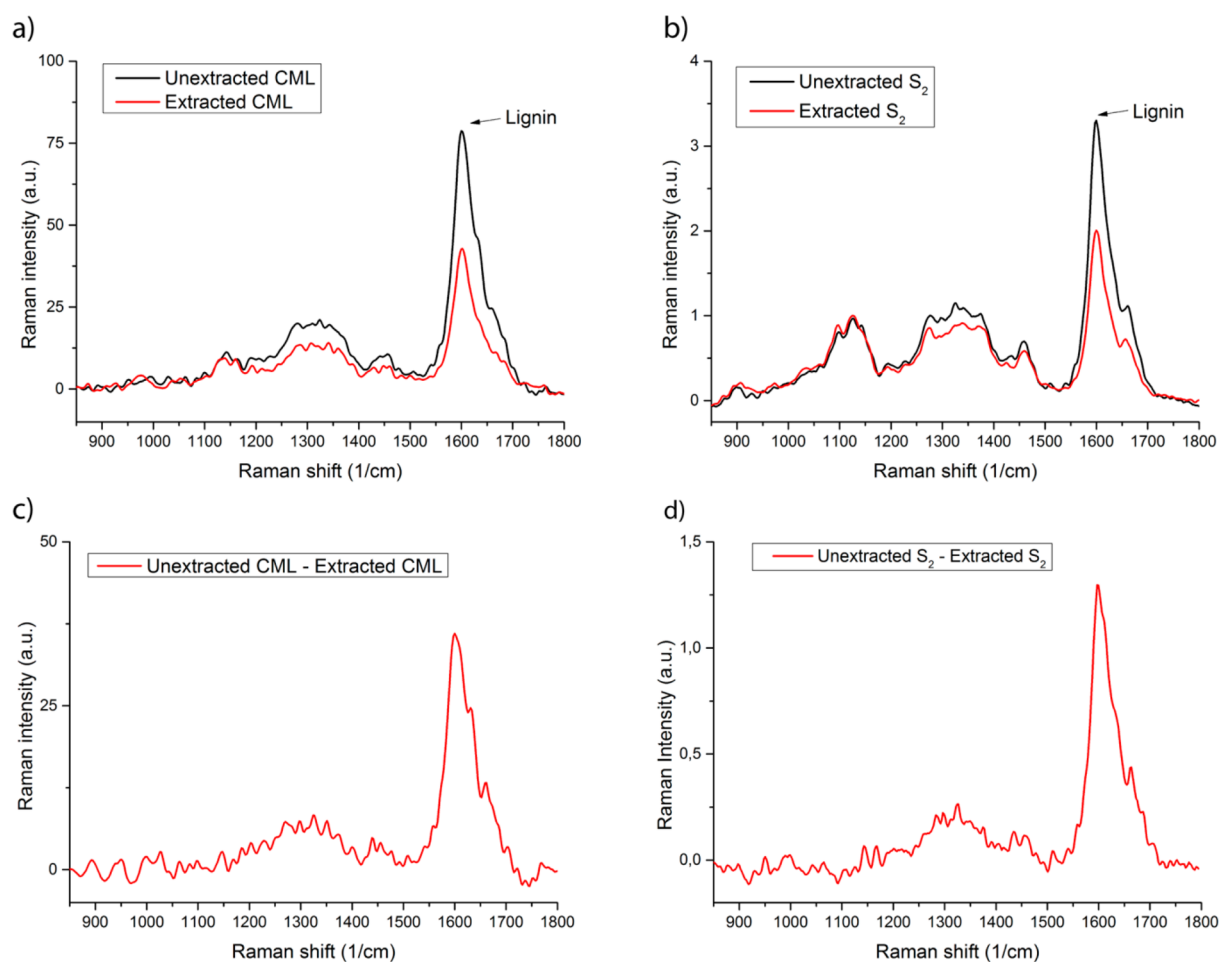


Figure 1. Average Raman spectra obtained from CML and S_2 layer of unextracted and extracted wood sections and their difference spectra: (a) average Raman spectra from CML (absolute), (b) normalized average Raman spectra from S_2 layer (relative to cellulose band at $\sim 1122\text{ cm}^{-1}$), (c) difference spectrum of unextracted and extracted CML in (a), and (d) difference spectrum of unextracted and extracted S_2 layer in (b).

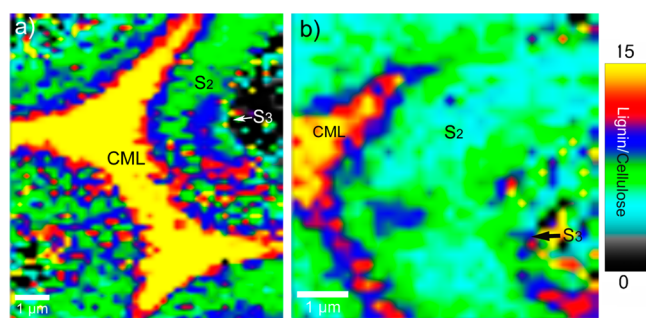


Figure 2. Raman images of transversely sectioned unextracted (a) and extracted (b) wood illustrating intensity ratio I_{1600}/I_{1122} (in secondary wall this corresponds to lignin/cellulose ratio). CML = Compound middle lamella.

chosen for this study was enough because we observed the progress of lignin extraction and the morphological location of residual lignin by examining ultrathin wood sections ($\sim 200\text{ nm}$). Although we could not image the same ROI before and after extraction, the information generated from this study can still enhance our understanding of the cell wall behavior during the lignin extraction process.

Transmission Electron Microscopy (TEM). TEM and KMnO_4 staining have been frequently used for studying lignin distribution in the wood cell wall. According to the degree of

lignification, the different cell wall layers show notable differences in their contrast after staining with KMnO_4 and can be visualized with TEM.^{15,34,35} TEM images of the unextracted (Figure 3) and extracted (Figure 4) Norway spruce wood cell wall were obtained after KMnO_4 staining to evaluate changes in the cell wall. Visual observation of the wood sections did not show significant differences after lignin

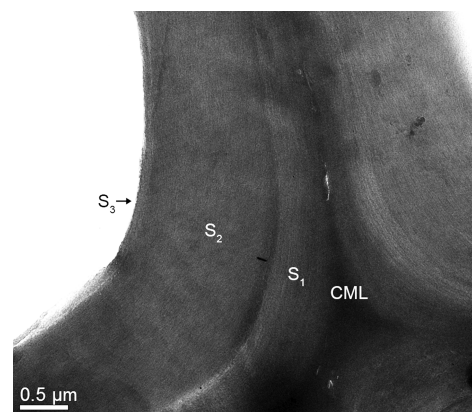


Figure 3. Transmission electron micrograph of unextracted wood section. Compound middle lamella (CML) region shows darker contrast after staining with KMnO_4 .

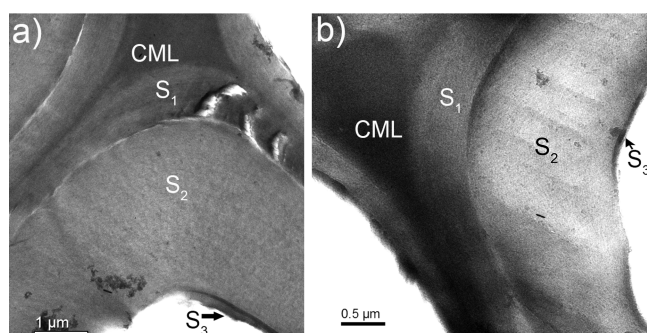


Figure 4. Transmission electron micrographs of 1 h extracted wood sections. In both images, compound middle lamella (CML) and S_3 layer are darkly contrasted after KMnO_4 staining.

extraction when compared with unextracted wood. However, TEM images of the unextracted sample showed a darkly stained CML with almost even staining of the other areas of the cell wall (Figure 3) corresponding to the results for softwood tracheids.³³ On the other hand, an intense staining was observed in the CML, cell corners, and S_3 layer of the extracted sample (Figure 4); in this case, the S_2 layer was also clearly less stained with KMnO_4 . The CML with dark contrast also became narrower after extraction. Our results correspond to an earlier study made by Maurer and Fengel¹² who studied the sources of milled wood lignin using TEM. After extraction, the presence of cracks in the S_1 layer across the cell wall and missing parts of secondary wall were observed (Figure 4). Because lignin acts as a binding polymer, which together with cellulose and hemicellulose makes the fibers stiff and rigid,³⁶ partial removal of cell wall lignin from ultrathin sections makes bonding weaker. Electron lucent and electron dense regions were found both in the fresh sections of Norway spruce³⁷ and in the S_2 layer post-extraction (Figure 4a), which illustrates a heterogeneous lignin distribution in the analyzed samples.

Our results clearly show that 1,4-dioxane can partly extract lignin not only from the middle lamella but also from the secondary wall, although the wood section is much thicker (~200 nm) than the dimensions of cellulose microfibrils (~3.5 nm). This is an unexpected observation as the cell wall is generally considered as a tightly packed composite from which the matrix of lignin and hemicellulose is physically difficult to remove. Additionally, lignin and hemicelluloses are partly associated with each other through covalent linkages forming lignin–carbohydrate complexes. For comparison, it is known that a fraction of the cell wall polysaccharides is solubilized during mechanical pulping of wood.³⁸ However, it is not likely that large amounts of lignin–hemicellulose complexes were extracted in our case because 1,4-dioxane is not a solvent for hemicellulose and also our samples were not mechanically preprocessed. The situation is presumably analogous to diblock copolymers where even a relatively small block of nondissolving component prevents dissolution in a solvent that would be a good solvent for the other block.

To summarize this work, study of the lignin-extracted ultrathin sections provides valuable information regarding cell wall behavior during extraction when all the layers are exposed to the extraction chemical. The concentration of lignin in all cell wall layers changed during the extraction process. However, lignin obtained after extraction consists mainly of secondary wall lignin as this area contains most of the total cell wall lignin in conifer tracheids. The presence of crack-like damage in the

S_1 layer of the secondary wall was observed after extraction. Both RM and TEM produced similar results. Further studies on the extracted material could provide us with more valuable information on the extraction process.

■ ASSOCIATED CONTENT

Supporting Information

Original ROIs where mappings were performed to produce images in Figure 2 and Raman images of transversely sectioned extracted and unextracted wood. This material is available free of charge via the Internet at <http://pubs.acs.org>.

■ AUTHOR INFORMATION

Corresponding Author

*Phone: +358 503442978. Fax: +358 9470 24259. E-mail: eero.kontturi@aalto.fi.

Notes

The authors declare no competing financial interest.

■ ACKNOWLEDGMENTS

This work was funded by the Multidisciplinary Institute of Digitalization and Energy (MIDE, <http://mide.aalto.fi>).

■ REFERENCES

- (1) Daniel, G. Wood and Fiber Morphology. In *Ljungberg Textbook: Pulp and Paper Technology*; Ek, M., Gellerstedt, G., Henriksson, G., Eds.; Fiber and Polymer Technology, KTH: Sweden: 2007; Book 1, pp 49–71.
- (2) Lawoko, M.; Henriksson, G.; Gellerstedt, G. Structural differences between the lignin–carbohydrate complexes present in wood and in chemical pulps. *Biomacromolecules* **2005**, *6*, 3467–3473.
- (3) Kamm, B.; Kamm, M.; Gruber, P.; Kromus, S. Biorefinery Systems: An Overview. In *Biorefineries – Industrial Processes and Products: Status Quo and Future Directions*; Kamm, B., Gruber, P., Kamm, M., Eds.; Wiley: Weinheim, Germany, 2006; Vol. 1, pp 3–40.
- (4) Chang, V. S.; Holtzapfel, M. T. Fundamental factors affecting biomass enzymatic reactivity. *Appl. Biochem. Biotechnol.* **2000**, *84–86*, 5–37.
- (5) Fan, L. T.; Lee, Y.-H.; Beardmore, D. R. The influence of major structural features of cellulose on rate of enzymatic hydrolysis. *Biotechnol. Bioeng.* **1981**, *23*, 419–424.
- (6) Ishizawa, C. I.; Jeoh, T.; Adney, W. S.; Himmel, M. E.; Johnson, D. K.; Davis, M. F. Can delignification decrease cellulose digestibility in acid pretreated corn stover? *Cellulose* **2009**, *16*, 677–686.
- (7) Ragauskas, A. J.; Nagy, M.; Kim, D. H.; Eckert, C. A.; Hallett, J. P.; Liotta, C. L. From wood to fuels: Integrating biofuels and pulp production. *Ind. Biotechnol.* **2006**, *2* (1), 55–65.
- (8) Gierlinger, N.; Keplinger, T.; Harrington, M. Imaging of plant cell walls by confocal Raman microscopy. *Nat. Protoc.* **2012**, *7*, 1694–1708.
- (9) Huang, F.; Singh, P. M.; Ragauskas, A. J. Characterization of milled wood lignin (MWL) in Loblolly pine stem wood, residue, and bark. *J. Agric. Food Chem.* **2011**, *59* (24), 12910–12916.
- (10) Mao, J.; Holtman, K. M.; Scott, J. T.; Kadla, J. F.; Schmidt-Rohr, K. Differences between lignin in unprocessed wood, milled wood, mutant wood, and extracted lignin detected by ^{13}C solid-state NMR. *J. Agric. Food Chem.* **2006**, *54* (26), 9677–9686.
- (11) Sorvari, J.; Sjöström, E.; Klemola, A.; Laine, J. E. Chemical characterization of wood constituents, especially lignin, in fractions separated from middle lamella and secondary wall of Norway spruce (*Picea abies*). *Wood Sci. Technol.* **1986**, *20* (1), 35–51.
- (12) Maurer, A.; Fengel, D. On the origin of milled wood lignin. *Holzforschung* **1992**, *46*, 471–475.
- (13) Agarwal, U. P.; Ralph, S. A. FT-Raman spectroscopy of wood: Identifying contributions of lignin and carbohydrate polymers in the

spectrum of black spruce (*Picea mariana*). *Appl. Spectrosc.* **1997**, *51*, 1648–1655.

(14) Hänninen, T.; Kontturi, E.; Vuorinen, T. Distribution of lignin and its coniferyl alcohol and coniferyl aldehyde groups in *Picea abies* and *Pinus sylvestris* as observed by Raman imaging. *Phytochemistry* **2011**, *72*, 1889–1895.

(15) Bland, D. E.; Foster, R. C.; Logan, A. F. The mechanism of permanganate and osmium tetroxide fixation and the distribution of lignin in the cell wall of *Pinus radiata*. *Holzforchung* **1971**, *25* (5).

(16) Agarwal, U. P. Raman imaging to investigate ultrastructure and composition of plant cell walls: distribution of lignin and cellulose in black spruce wood (*Picea mariana*). *Planta* **2006**, *224*, 1141–1153.

(17) Gierlinger, N.; Schwanninger, M. The potential of Raman microscopy and Raman imaging in plant research. *Plant Physiol.* **2007**, *21*, 69–89.

(18) Ma, J.; Zhang, Z.; Yang, G.; Mao, J.; Xu, F. Ultrastructural topochemistry of cell wall polymers in *Populus nigra* by transmission electron microscopy and Raman imaging. *BioResources* **2011**, *6* (4), 3944–3959.

(19) Atalla, R. H.; Agarwal, U. P. Raman microprobe evidence for lignin orientation in the cell walls of native woody tissue. *Science* **1985**, *227*, 636–638.

(20) Atalla, R. H.; Whitmore, R. E.; Heimbach, C. J. Raman spectral evidence for molecular-orientation in native cellulose fibres. *Macromolecules* **1980**, *13*, 1717–1719.

(21) Gierlinger, N.; Luss, S.; König, C.; Konnerth, J.; Eder, M.; Fratzl, P. Cellulose microfibril orientation of *Picea abies* and its variability at the micron-level determined by Raman imaging. *J. Exp. Bot.* **2010**, *61* (2), 587–595.

(22) Agarwal, U. P.; Ralph, S. A. Determination of ethylenic residues in wood and in TMP of spruce by FT-Raman spectroscopy. *Holzforchung* **2008**, *62*, 667–675.

(23) Nuopponen, M.; Willför, S.; Jääskeläinen, A.-S.; Sundberg, A.; Vuorinen, T. A UV resonance Raman (UVR) spectroscopic study on the extractable compounds in Scots pine (*Pinus sylvestris*) wood. Part I: lipophilic compounds. *Spectrochim. Acta, Part A* **2004**, *60*, 2953–2961.

(24) Nuopponen, M.; Willför, S.; Jääskeläinen, A.-S.; Vuorinen, T. A UV resonance Raman (UVR) spectroscopic study on the extractable compounds in Scots pine wood (*Pinus sylvestris*). Part II: hydrophilic compounds. *Spectrochim. Acta, Part A* **2004**, *60*, 2963–2968.

(25) Saariaho, A.-M.; Hortling, B.; Jääskeläinen, A.-S.; Tamminen, T.; Vuorinen, T. Simultaneous quantification of residual lignin and hexenuronic acid from chemical pulps with UV resonance Raman spectroscopy and multivariate calibration. *J. Pulp. Pap. Sci.* **2003**, *29*, 363–370.

(26) Saariaho, A.-M.; Jääskeläinen, A.-S.; Nuopponen, M.; Vuorinen, T. Ultra-violet resonance Raman spectroscopy in lignin analysis: determination of characteristic vibrations of p-hydroxyphenyl, guaiacyl, and syringyl lignin structures. *Appl. Spectrosc.* **2003**, *57*, 58–66.

(27) Lewis, N. G.; Yamamoto, E. Lignin: Occurrence, biogenesis and biodegradation. *Annu. Rev. Plant Physiol. Plant Mol. Biol.* **1990**, *41*, 455–496.

(28) Chiang, V. L.; Funaoka, M. The dissolution and condensation reactions of guaiacyl and syringyl units in residual lignin during kraft delignification of sweetgum. *Holzforchung* **1990**, *44*, 147–155.

(29) Khalil, H. P. S. A.; Yusra, A. F. I.; Bhat, A. H.; Jawaid, M. Cell wall ultrastructure, anatomy, lignin distribution, and chemical composition of Malaysian cultivated kenaf fiber. *Ind. Crops Prod.* **2010**, *31*, 113–121.

(30) Xu, F.; Zhong, X. C.; Sun, R. C.; Lu, Q. Anatomy, ultrastructure and lignin distribution in cell wall of *Caragana korshinskii*. *Ind. Crops Prod.* **2006**, 186–193.

(31) Holmbom, B.; Eckerman, C.; Eklund, P.; Hemming, J.; Nisula, L.; Reunanen, M.; Sjöholm, R.; Sundberg, A.; Sundberg, K.; Willför, S. Knots in trees – A new rich source of lignans. *Phytochem. Rev.* **2003**, *2*, 331–340.

(32) Willför, S.; Hemming, J.; Reunanen, M.; Eckerman, C.; Holmbom, B. Lignans and lipophilic extractives in Norway spruce knots and stemwood. *Holzforchung* **2003**, *57*, 27–36.

(33) Sjöström, E. *Wood Chemistry Fundamentals and Applications*; Academia Press, Inc.: London, 1981; p 223.

(34) Lehringer, C.; Daniel, G.; Schmitt, U. TEM/FE-SEM studies on tension wood fibres of *Acer* spp., *Fagus sylvatica* L. and *Quercus robur* L. *Wood Sci. Technol.* **2009**, *43*, 691–702.

(35) Maurer, A.; Fengel, D. A new process for improving the quality and lignin staining of ultrathin sections from wood tissues. *Holzforchung* **1990**, *44*, 453–460.

(36) Henriksson, G. Lignin. In *Ljungberg Textbook: Pulp and Paper Technology*; Ek, M., Gellerstedt, G., Henriksson, G., Eds.; Fiber and Polymer Technology, KTH; Sweden, 2007; Book 1, pp 125–148.

(37) Singh, A. P.; Daniel, G. The S2 layer in the tracheid walls of *Picea abies* wood: Inhomogeneity in lignin distribution and cell wall microstructure. *Holzforchung* **2001**, *55*, 373–378.

(38) Thornton, J.; Ekman, R.; Holmbom, B.; Örså, F. Polysaccharides dissolved from Norway spruce in thermomechanical pulping and peroxide bleaching. *J. Wood Chem. Technol.* **1994**, *14* (2), 159–175.